Device Physics of Organic TFTs

2009. 6. 2

Changhee Lee
School of Electrical Engineering and Computer Science
Seoul National Univ.
chlee7@snu.ac.kr

Organic Thin-Film Transistor

Top-contact OTFT 구조

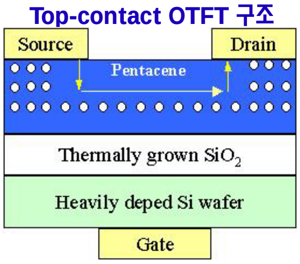

다양한 종류의 TFT 비교

a-Si:H	LTPS	Organic
• low mobility (~1 cm^2/Vs) • matured tech. • process temp. (<150 °C) • instability	• high mobility (> 10 cm^2/Vs) • non-uniform for large area • process temp. (<150 °C) • high stability	• low~medium mobility (<10 cm^2/Vs) • process temp. (<100 °C) • patterning, stability prob.

OTFT의 장점

- 간단한 제작 공정
  : vacuum deposition, spin-coating, ink-jet printing, roll-to-roll, …
  ➔ 저온/저비용/대면적 공정 가능
- 다양한 기판 사용 가능
  : wafer, glass, plastic, foil, …
  ➔ 다양한 회로에 응용 가능

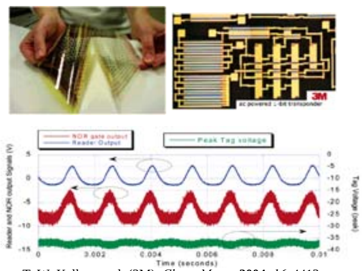

T. W. Kelley, et al. (3M), *Chem. Mater.* **2004,** *16,* 4413

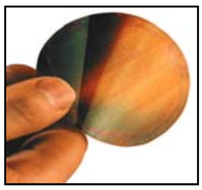

Philips (1998)

Status of OTFT performances and printable organic semiconductors

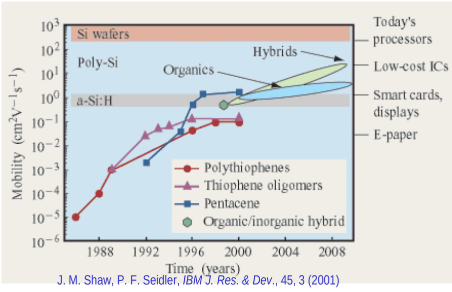

J. M. Shaw, P. F. Seidler, *IBM J. Res. & Dev.*, 45, 3 (2001)

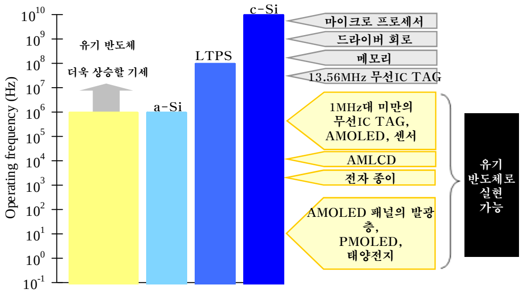

Nikkei Electronics Asia 2001년12월호

Material	mobility (cm^2/Vs)	on/off ratio	reference
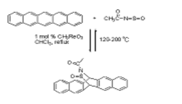	0.89	-	A. Afzali, et. al., J. Am. Chem. Soc.2002, 124, 8812.
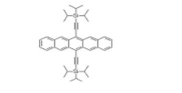	0.4	10^6	Sheraw et al., Adv. Mater., 2003, 15, 2009
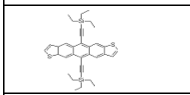	1	10^7	J. E. Anthony et al., J. Am. Chem. Soc., 2005, 127, 4986.
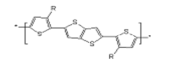	0.2 ~ 0.6	10^7	I. McCulloch, et al. Nat. Mater. 5. 328 (2006)
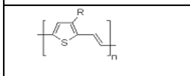	0.22	-	H. Fuchigami et. al., Appl. Phys. Lett., 63, 1372 (1993)
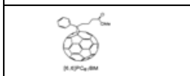	0.02 ~ 0.1	10^4	Tae-Woo Lee, et al., Adv. Mater. 17, 2180 (2005)

OTFT: Basic Principle

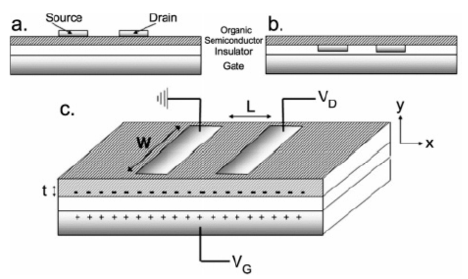

Figure 1. Schematic of top (a) and bottom (b) contact organic TFTs. (c) Relevant voltages and geometry for a TFT.

Areal density of charge (C/cm^2) induced at a given position x along the channel:

$$q_{ind}(x) = n(x)et = C_{ox}(V_G - V_T - V(x))$$

C_{ox} = capacitance of the insulator per unit area, (nF/cm^2)

$n(x)$ = number density of charges in the channel ($no./cm^3$)

e = fundamental unit of charge

t = thickness of the charged layer in the channel.

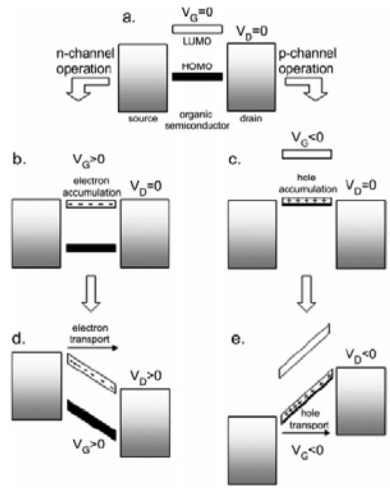

Figure 2. (a) Idealized energy level diagram of an organic TFT at $V_G = 0$ and $V_D = 0$. (b−e) demonstrate the principle of field effect transistor operation for the case of electron accumulation (b) and transport (d) and hole accumulation (c) and transport (e).

Christopher R. Newman, C. Daniel Frisbie, Demetrio A. da Silva Filho, Jean-Luc Bre´das, Paul C. Ewbank, and Kent R. Mann, *Chem. Mater.* **2004,** *16,* 4436-4451

OTFT: Basic Principle

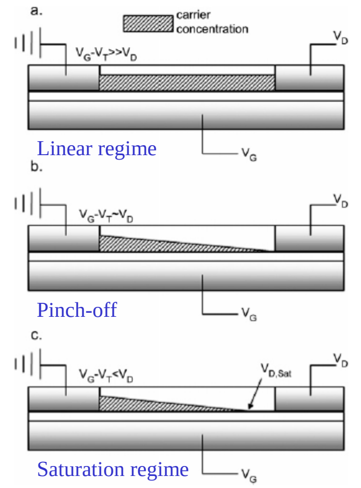

Figure 4. (a) Carrier concentration profile of TFT in the linear regime. (b) Pinch-off occurs when $V_D \approx V_G - V_T$. (c) Carrier concentration profile of TFT in the saturation regime.

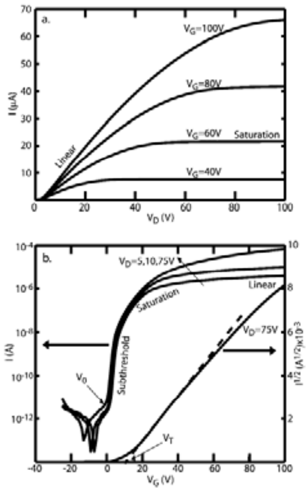

Figure 3. (a) Example I_D-V_D curves for a PTCDI-C₈ TFT for various values of V_G. (b) Example I_D-V_G curves plotted on semilogarithmic axes for the same device for various values of V_D. The $I^{1/2}$ vs V_G curve for V_D = 75V is shown on the right-hand axis.

- **Nonzero V_G (=V_{FB}) is generally needed in order to achieve the flat-band condition** due to a mismatch between the Fermi level of the metal and the LUMO (or HOMO) of organic semiconductor.

- **Threshold gate voltage, V_T, is necessary to induce mobile charges.**
  - If there are large numbers of deep electron (or hole) traps present in the film, these will have to be filled before the channel can conduct.
  - If the channel is inadvertently doped with charged carriers, it will be conductive at V_G =0.

- For an n-channel material,
  - doping the channel shifts V_T negatively (The device has to be biased negatively to shut it off).
  - deep traps shift V_T positively.

Christopher R. Newman, C. Daniel Frisbie, Demetrio A. da Silva Filho, Jean-Luc Bre´das, Paul C. Ewbank, and Kent R. Mann, *Chem. Mater.* **2004,** *16,* 4436-4451

Operation characteristics in a linear region

- **Linear region** ($V_D \ll V_G$)

$$I_D = \frac{W}{L} C_{ox} \mu (V_G - V_T - \frac{V_D}{2}) V_D$$

Linear regime : $V_G - V_T >> V_D$

Source	Organic Semiconductor	Drain
	Gate Insulator	
	Gate	
	Substrate	

$$\text{Ohm's Law}: \frac{I_D}{tW} = \sigma \frac{V_D}{L} \Rightarrow I_D = \frac{W}{L}(n_{ind,av} et)\mu V_D$$

$$q_{ind,av} = n_{ind,av} et = C_{ox}(V_G - V_T - \frac{V_D}{2})$$

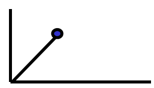

$$I_D = \frac{W}{L} C_{ox}\mu[(V_G - V_T) - \frac{V_D}{2}]V_D$$

$$= \frac{W}{L} C_{ox}\mu[(V_G - V_T)V_D - \frac{V_D^2}{2}]$$

$$\frac{\partial g_m}{\partial V_D} = \frac{\partial g_d}{\partial V_G} = \frac{W}{L} C_{ox}\mu_{lin}$$

$$\text{Transconductance}: g_m = \frac{\partial I_D}{\partial V_G}|_{V_D} = \frac{W}{L} C_{ox}\mu_{lin} V_D$$

$$\text{Conductance}: g_d = \frac{\partial I_D}{\partial V_D}|_{V_G} \sim \frac{W}{L} C_{ox}\mu_{lin}(V_G - V_T) \text{ when } (V_G - V_T) >> V_D.$$

Operation characteristics in a saturation region

❑ **Saturation region** ($V_D \gg V_G$)

$$V_D = V_G - V_T; \quad \Rightarrow I_D = \frac{W}{L} C_{ox}\mu_{sat}[(V_G - V_T)V_D - \frac{V_D{}^2}{2}]$$

$$I_D = \frac{W}{2L} C_{ox}\mu_{sat}(V_G - V_T)^2$$

$$\boxed{I_{D,sat} = \frac{W}{2L} C_{ox}\mu_{sat}(V_G - V_T)^2}$$

- μ_{sat} can be calculated from the slope of a line through the linear part of an $I_{D,sat}^{1/2}$ vs V_G plot
- V_T can be calculated from the intercept of a line through the linear part of an $I_{D,sat}^{1/2}$ vs V_G plot.

Saturation regime : $V_G - V_T < V_D$

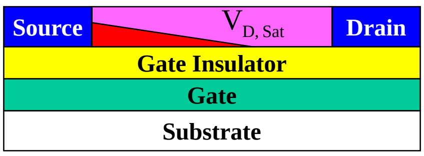

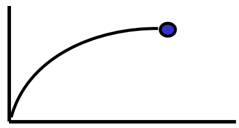

Operation characteristics of OTFTs

- **Often $\mu_{saturation}$ is higher than μ_{linear} .**

As V_G is increased, more of traps are filled and unavailable to trap subsequent carriers.
→ The mobility in the saturation region appears to be a continuously increasing function of V_G.

Bassler's Gaussian disorder model

$$\mu(F,T) = \mu_\infty \exp\left[-\left(\frac{2\sigma}{3k_B T}\right)^2\right]\exp\left\{C\left[\left(\frac{\sigma}{k_B T}\right)^2 - \Sigma^2\right]\sqrt{F}\right\}$$

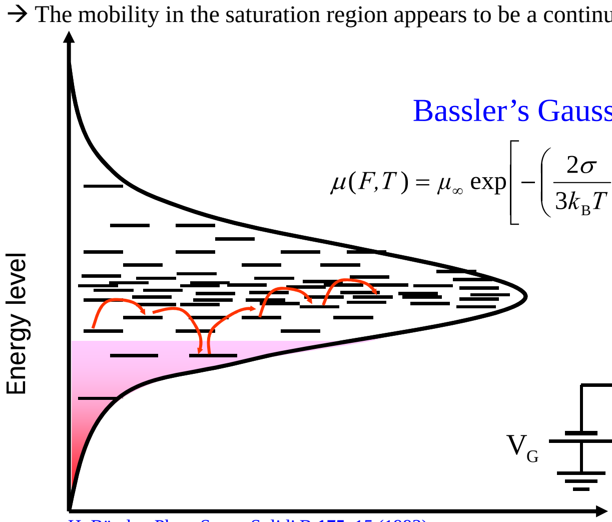

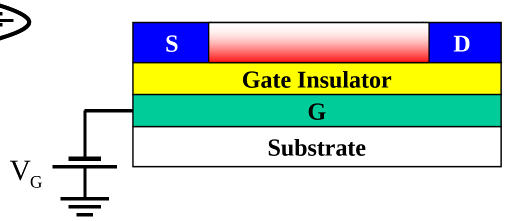

H. Bässler, Phys. Status Solidi B **175**, 15 (1993).

Operation characteristics of OTFTs

• **Contact resistances**: nonnegligible voltage drops near the contacts due to Schottky barriers and (in the case of top-contact devices) resistances through the ungated portion of the organic semiconductor are almost invariably present in these devices. Contact resistances are likely to be less noticeable in the saturation region since the integrated resistance of the channel is higher than in the linear region.

• **Offset between V_o and V_T** : V_T, calculated from the intercept of a line drawn through the linear region of $I_{D,sat}^{1/2}$ vs V_G plot, does not coincide with the exponential increase in current (V_o) due to traps in the active layer. In general, the higher the mobility of the device, the smaller this offset is, since high trap concentrations cause low mobilities and large offsets.

• **On/off current ratio**: $\frac{I_{ON}}{I_{OFF}}$

Maximizing the mobility generally leads to a high on/off ratio since μ determines I_{ON}.

• **Subthreshold swing S (V/decade or mV/decade)** : $S = \frac{dV_G}{d(\log I_D)}$

S is a measure of how rapidly the device switches from the off state to the on state. A large S generally implies a large concentration of shallow traps, i.e., a diffuse turn-on region.

Dependence of the threshold voltage on doping and gate insulator thickness

Organic Semiconductor
EE 4541.617A
2009. 1st Semester

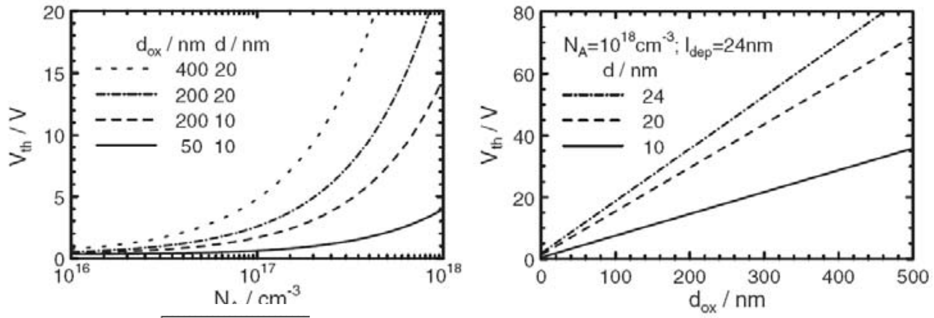

$$l_{\rm dep} = \sqrt{\frac{2\epsilon\epsilon_0|2\varphi_{\rm b}|}{e}\,N_{\rm A}^-}\,, \qquad \varphi_{\rm b} = -V_{\rm T}\ln\frac{N_{\rm A}^-}{n_{\rm i}}$$

$$V_{\rm th} = V_{\rm FB} + \frac{eN_{\rm A}^- d}{C''_{\rm ox}} - 2\varphi_{\rm b}\left(\frac{d}{l_{\rm dep}}\right), \qquad d < l_{\rm dep}$$

$$V_{\rm FB} = \Phi_{\rm MS} - \frac{Q''_{\rm if}}{C''_{\rm ox}} = \Phi_{\rm MS} - \frac{eN''_{\rm if}d_{\rm ox}}{\epsilon_0\epsilon_{\rm ox}}$$

• S. Scheinert and G. Paasch, phys. stat. sol. (a) **201**, 1263, (2004)

Changhee Lee, SNU, Korea

Mobility Measurement Techniques: TRM-SHG

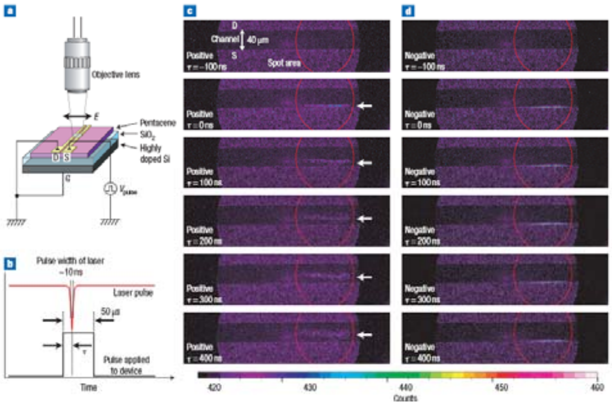

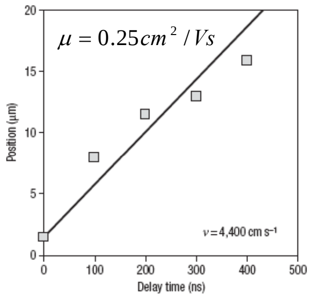

T. Manaka, E. Lim, R. Tamura, M. Iwamoto, *Nature Photon.* **1,** 581 (2007).

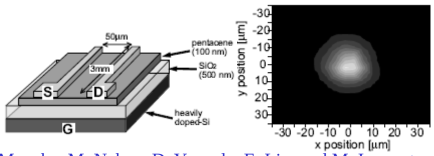

$$I(2\omega) \propto \left|\chi^{(3)}(2\omega;0,\omega,\omega)E(0)E(\omega)E(\omega)\right|^2$$

$$I_{2\omega}(x) \propto \left|\int_{-\infty}^{\infty} E(\xi) I_\omega(x-\xi)\, d\xi\right|^2$$

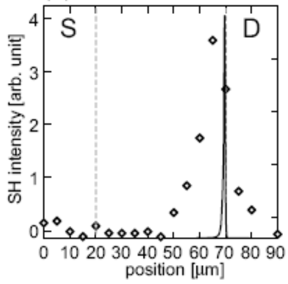

T. Manaka, M. Nakao, D. Yamada, E. Lim and M. Iwamoto, Optics Express 15, 15964 (2008).

Important factors to affect OTFT performances

Organic semiconductors
- High mobility
- High stability
- Processibility

Gate Insulators
- High gate capacitance
- Low leakage current
- High breakdown voltage

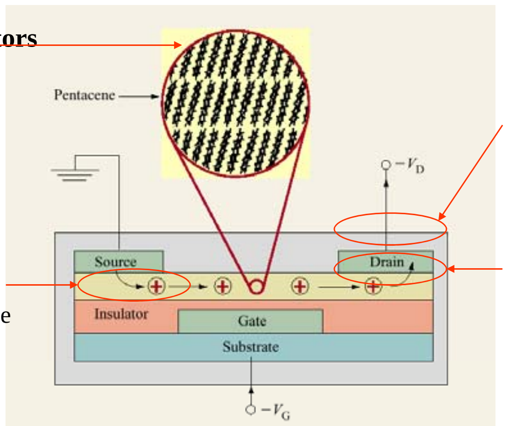

Contact
- Ohmic
- Low contact resistance
- Low parasitic capacitance

Interface
- Crystallinity/Directionality control
- Low trap density
- Stability and uniformity

Active materials: Organic semiconductors

Organic Semiconductor
EE 4541.617A
2009. 1st Semester

Semiconductor	Representative chemical structure	Mobility ($cm^2 V^{-1} s^{-1}$)
Silicon	Silicon crystal	300–900
	Polysilicon	50–100
	Amorphous silicon	~1
Pentacene	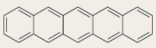	~1
α,ω-dihexyl-sexithiophene	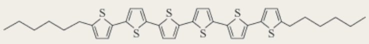	10^{-1}
α,ω-dihexylanthra-dithiophene	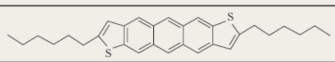	10^{-1}
Regioregular poly(3-hexylthiophene)	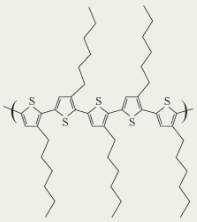	10^{-1}
Organic–inorganic hybrid	Phenethylamine–tin iodide	~1

J. M. Shaw, P. F. Seidler, *IBM J. Res. & Dev.*, **45**, 3 (2001)

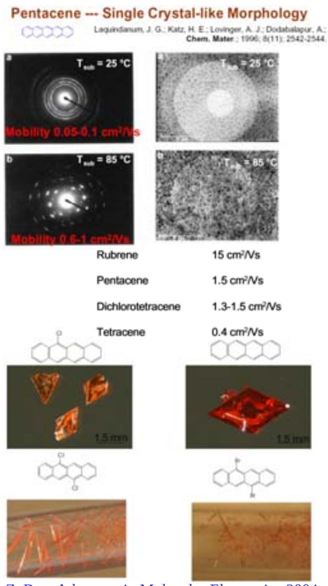

Z. Bao, Advances in Molecular Electronics 2004

Changhee Lee, SNU, Korea

Correlation between morphology and mobility

Organic Semiconductor
EE 4541.617A
2009. 1st Semester

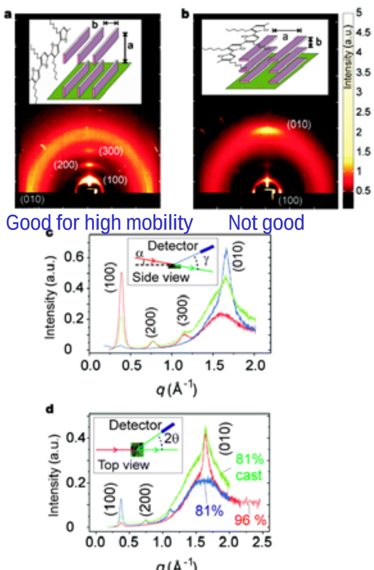

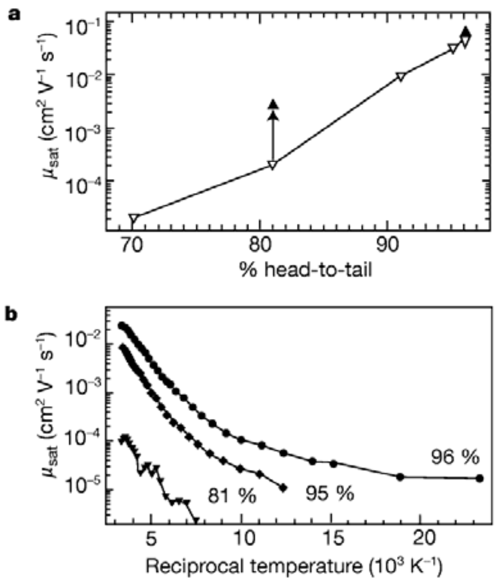

H. Sirringhaus et al. *Nature* 401, 685 – 688 (1999)

Changhee Lee, SNU, Korea

Effect of crystallization on the mobility

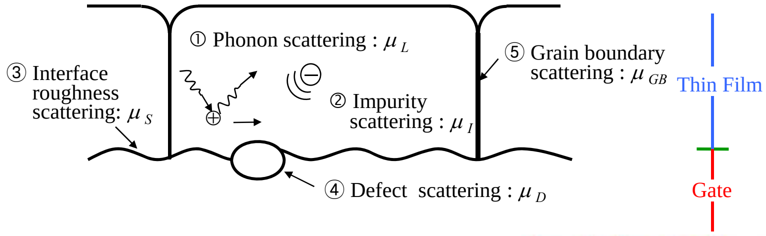

$$\frac{1}{\mu} = \frac{1}{\mu_L} + \frac{1}{\mu_I} + \frac{1}{\mu_S} + \frac{1}{\mu_D} + \frac{1}{\mu_{GB}}$$

$$= \frac{1}{\mu_B} + \frac{1}{\mu_{GB}}$$

$$\boxed{\frac{1}{\mu_B} << \frac{1}{\mu_{GB}}}$$

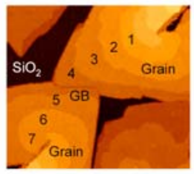

Conducting Probe AFM on
a pair of oligothiophene grains

J. Phys. Chem., 2001

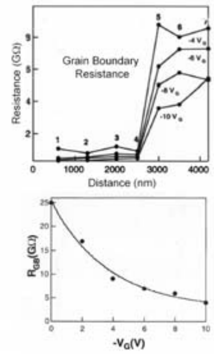

김성현박사 (ETRI) KAIST-EMDEC 발표자료

Role of Grain Boundaries

Donor-like grain boundary conduction model applied to p-channel TFT

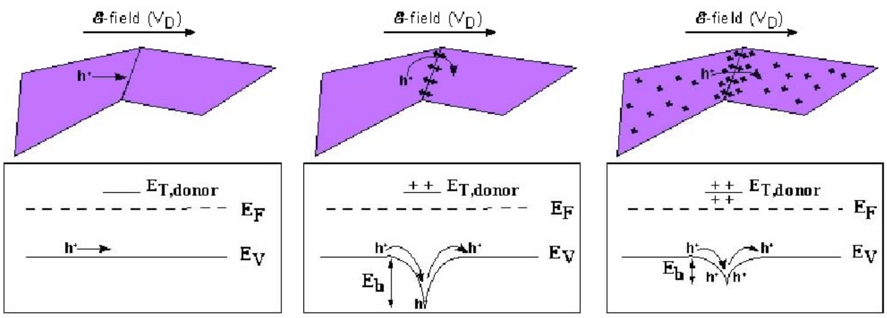

TFT in 'Off-State'
$V_G << V_T$

Before GB Charging
Energy Barrier has not formed yet.

TFT turning 'On'
$V_G \sim V_T$

GB has charged fully
Energy Barrier is maximum.

TFT fully 'On'
$V_G > V_T$

GB is screened by bound holes
Energy Barrier is decreasing.

Model developed by Seager, C.H., et. al., *J. App. Phys.*, **49**, 3879 (1978).

Grain boundary transport

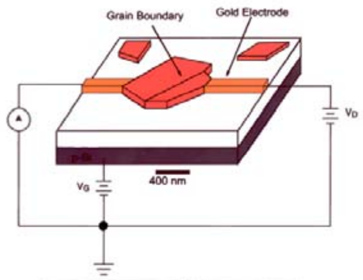

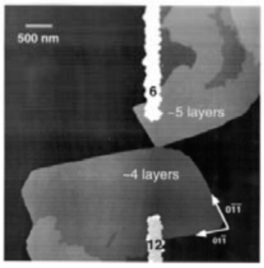

Activated, Gate Voltage Dependent!

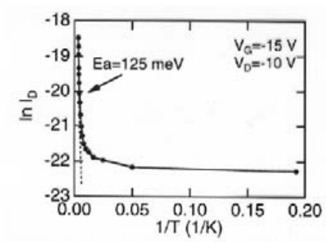

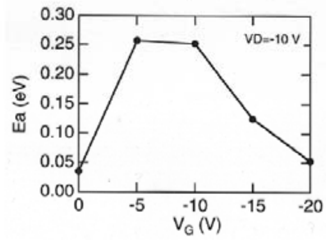

C. Daniel Frisbie, NSF Workshop Organic Electronics 2003. 1. 16-17

Gate insulator: High dielectric constant

Organic Semiconductor
EE 4541.617A
2009. 1st Semester

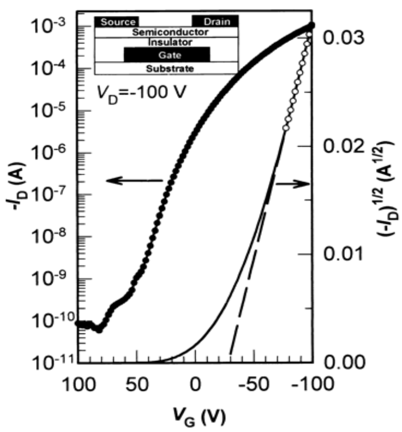

500 nm SiO_2 gate dielectrics

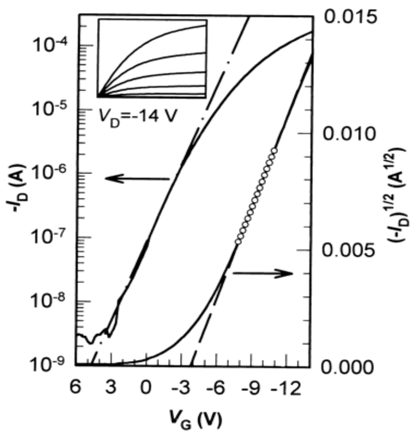

122 nm BZT gate dielectrics

C. D. Dimitrakopoulos, et.al., Science **283**, 822 (1999).

Gate insulator: low thickness using SAM

Organic Semiconductor
EE 4541.617A
2009. 1st Semester

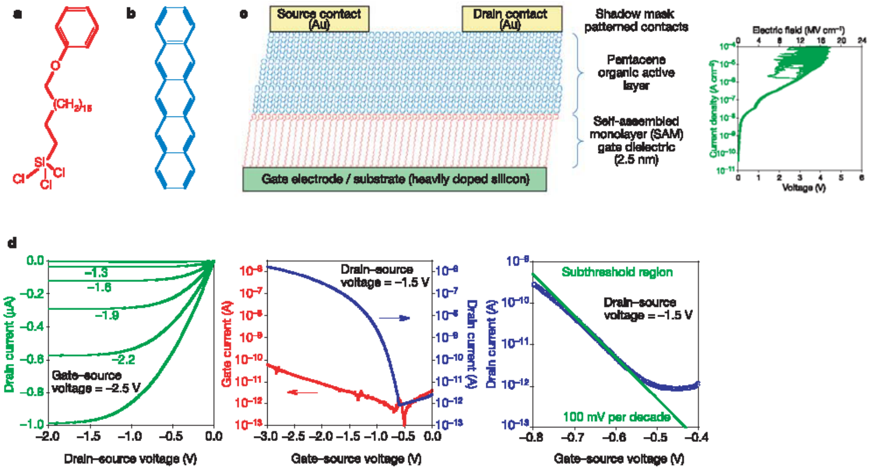

Figure 1 Chemical structures of organic materials, and cross-section and electrical characteristics of a TFT with molecular SAM gate dielectric. **a**, Structure of (18-phenoxyoctadecyl)trichlorosilane (PhO-OTS). **b**, Structure of the organic semiconductor pentacene. **c**, Cross-section of a pentacene TFT with SAM dielectric and source/drain contacts deposited through a shadow mask. **d**, Output characteristics; **e**, transfer characteristics; **f**, subthreshold region, showing a subthreshold swing of 100 mV per decade.

Marcus Halik, et al. (Infineon Technologies), Nature **431**, 963 (2004)

Changhee Lee, SNU, Korea

P3HT OTFTs with a SAM interface

Organic Semiconductor
EE 4541.617A
2009. 1st Semester

Polythiophene transistors

- Xerox polythiophene
  - Regioregular
  - polycrystalline
- SAM to increase mobility
- Hole conduction, 300K mobility ~0.1 cm^2/Vs
- Coplanar contacts

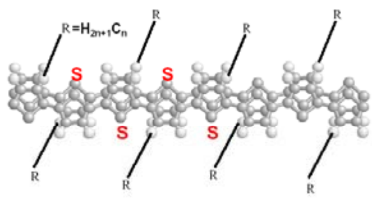

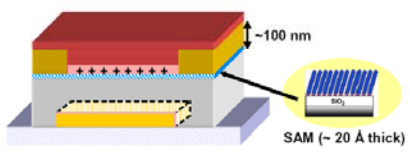

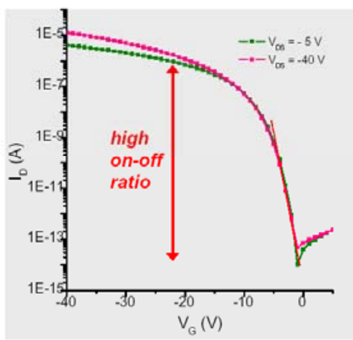

R. S. Street (Xerox)

Changhee Lee, SNU, Korea

Contact Resistance

Contact resistance $R_{total} = \sum R_{contacts} + R_{channel}$

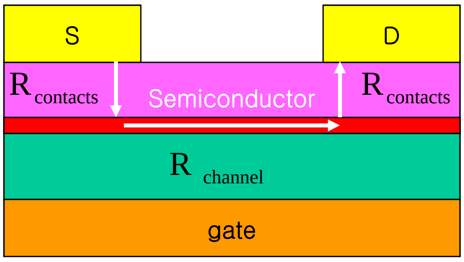

- **Origin of contact resistance**

- Schottky barrier: Mismatch between the Fermi level of the metal and the organic LUMO (or HOMO)
→ charge transfer between the metal and organic, causing a dipole and band bending in the organic semiconductor.

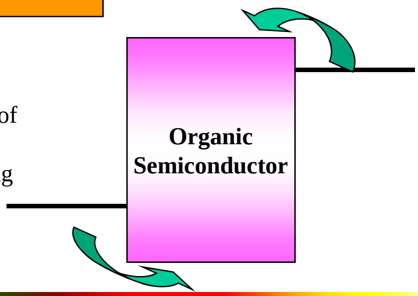

- Morphological defects at the interfaces.

Contact resistance: potentiometry experiment

Kelvin probe force microscopy demonstrated that the measured potential reflects the electrostatic potential of the accumulation layer at the semiconductor/insulator interface.

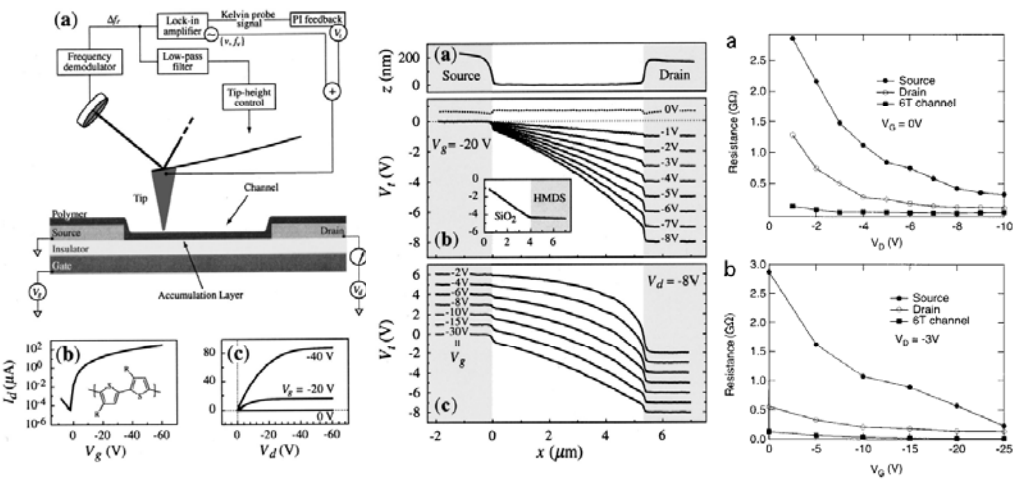

K. Seshadri and C. Daniel Frisbie, Appl. Phys. Lett., **78**, 993 (2001)

Reliability of OTFTs

Understanding stress and environmental effects is essential for circuit design and display packaging

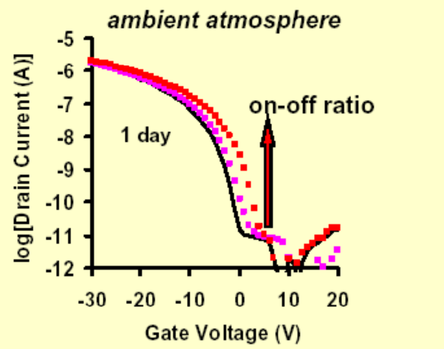

Ambient exposure decreases on-off ratio (reversible with heating)

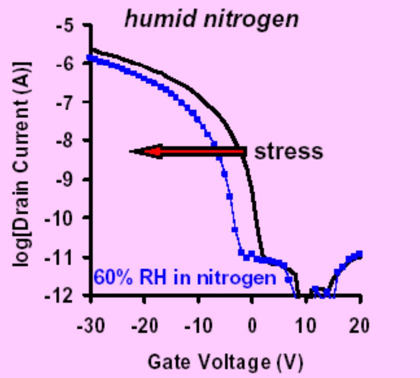

Humidity causes strong bias stress (reversible with heating)

R. S. Street (Xerox)

Bias stress in organic thin-film transistors

Organic Semiconductor
EE 4541.617A
2009. 1st Semester

All-organic TFTs based on the solution-processed semiconductor pentacene, in which the electrodes were manufactured from polyaniline and the insulator from a commercial photoresist

Threshold voltage shifts after application of a constant bias stress were measured in the linear regime, i.e., with the gate voltage being much larger than the voltage between the drain and source

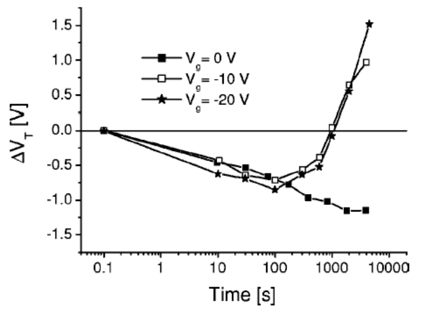

FIG. 1. Threshold voltage shift ΔV_T as a function of time and gate bias V_g at a fixed source drain–source bias of $V_{ds} = -10$ V.

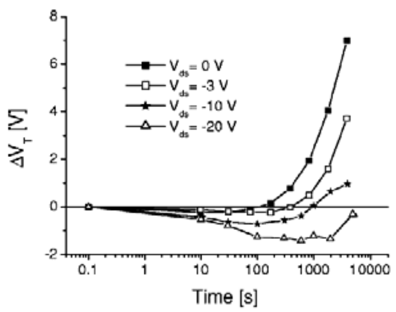

FIG. 2. Threshold voltage shift ΔV_T as a function of time and drain–source bias V_{ds} at a fixed gate bias of $V_g = -10$ V.

• Positive ΔV_T for negative gate bias stress: mobile ions drifting in the insulator when a gate field is applied. Trapping of charge carriers at the semiconductor–insulator interface plays only a minor role.

S. J. Zilker, C. Detcheverry, E. Cantatore, and D. M. de Leeuw, Appl. Phys. Lett., **79**, 1124 (2001)

Bias stress in organic thin-film transistors

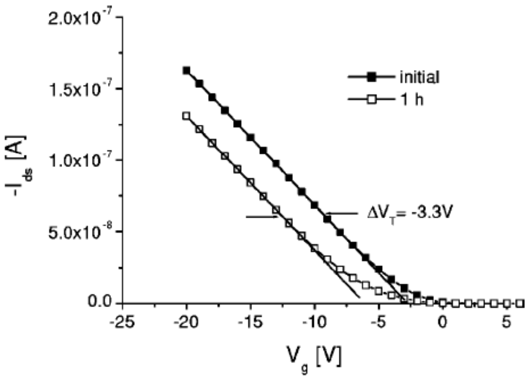

FIG. 3. Gate sweeps of a pentacene TFT measured in vacuum after annealing at 50 °C. The device was stressed for 1 h at $V_g = -10$ V and $V_{ds} = -1$ V. A threshold shift of -3.3 V is observed.

• Positive ΔV_T : Water absorption in the insulator may be its origin.

To eliminate possible water effects, stress measurements were carried out in vacuum with samples which were annealed at 50 ˚C for several hours. Under these conditions, no positive shift is observed.

• ΔV_T is purely negative, → charge trapping.

S. J. Zilker, C. Detcheverry, E. Cantatore, and D. M. de Leeuw, Appl. Phys. Lett., **79**, 1124 (2001)

Organic electronics: applications

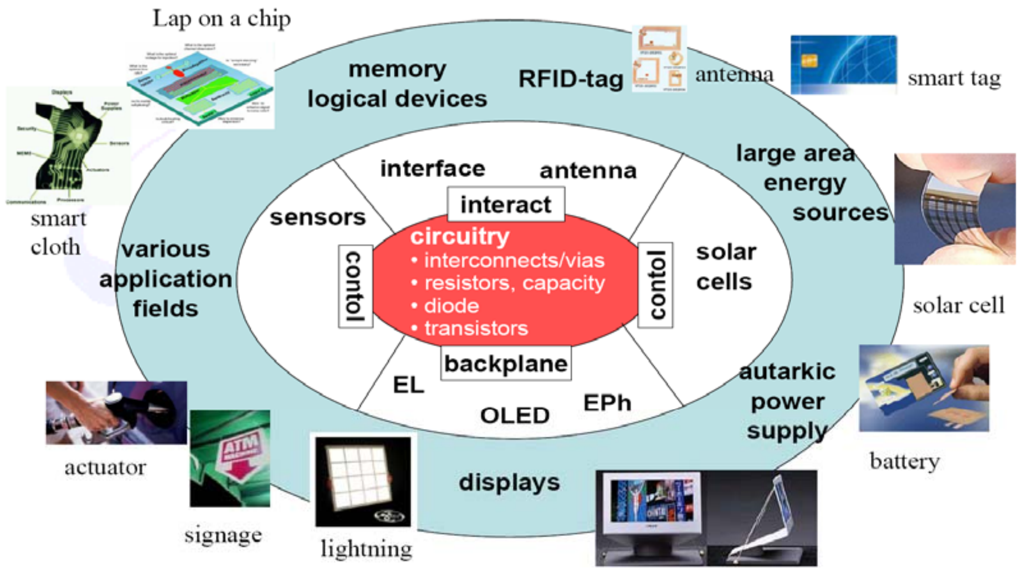

A. C. Huebler, *Printed Electronics Europe 06, Cambridge, 2006.*

Flexible displays

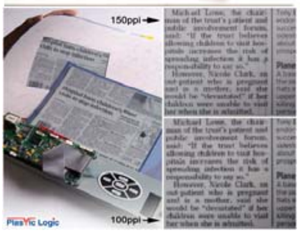

Plastic Logic 150ppi and 100ppi flexible active-matrix displays using E Ink Imaging Film.

- Global market revenue for flexible display panels will reach $339 million in 2013, rising at a compound annual growth rate (CAGR) of 83.5% from $5 million in 2006.
- Market revenue will break the landmark $100 million level in 2011. Unit shipments will rise to 198 million in 2013, up from 364,000 in 2006.

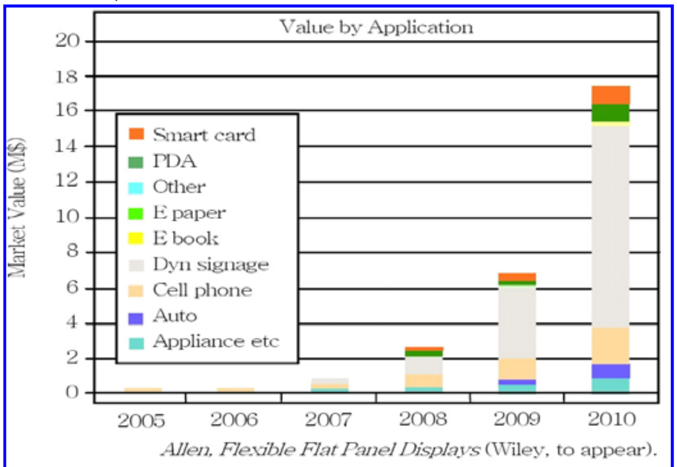

Flexible Display Market

Printed electronics: cell phones and Smart card

Nokia Aeon concept phone

Nokia 888 Concept Phone

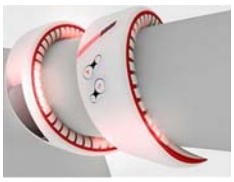

BenQ Siemens Snake phone

NEC Tag concept phone

RFID

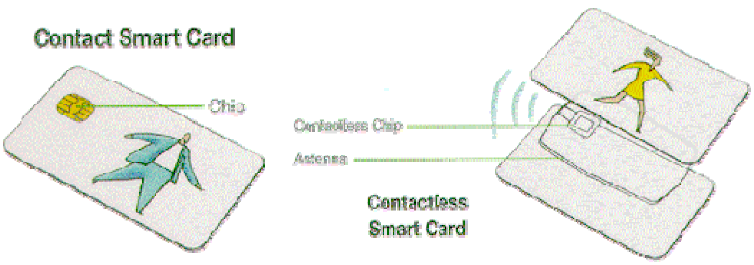

OTFT Application: RFID

- **Radio frequency identification (RFID) is a very broadbased technology that encompasses many application areas where identification, verification, tracking, and/or general logistics are important.**
- **An RFID system is generally comprised of a single reader instrument and many transponder circuits (tags). The transponders are attached to an article that needs to be identified.**
- **The reader and transponder communicate, typically with near-field or far-field electromagnetic coupling.**

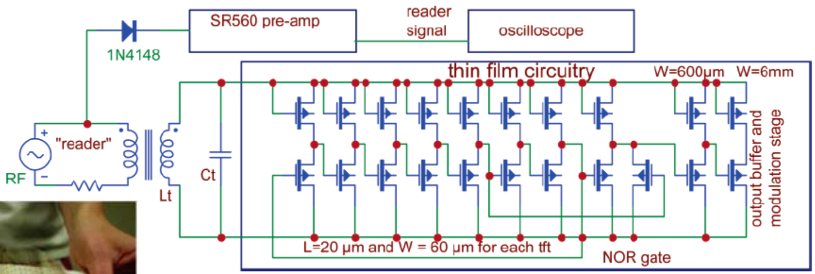

Circuit diagram of ac-powered one-bit rf transponder circuitry

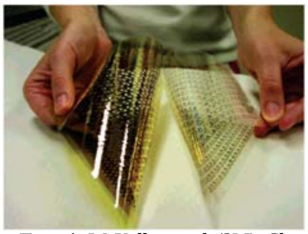

Optical image of 6 in 6 in RFID circuit array (right) fabricated on polymeric substrate, via the polymeric shadow mask shown at left.

Tommie W. Kelley, et al. (3M), *Chem. Mater.* 2004, *16*, 4413-4422

OTFT Application: RFID

Organic Semiconductor
EE 4541.617A
2009. 1st Semester

Optical micrograph of pentacene-based one-bit rf transponder circuit fabricated according to the ac-powering design, showing the seven-stage ring oscillator, an NOR gate, and two output invertors

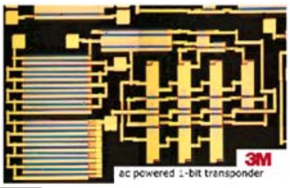

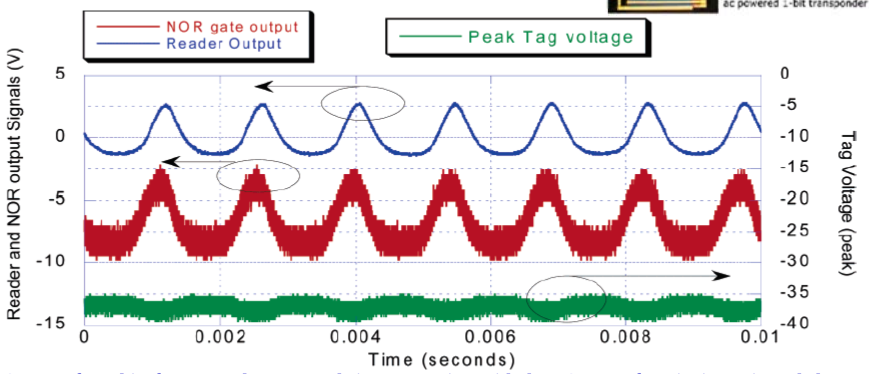

Output of one-bit rf transponder, operated via ac powering, with the NOR gate functioning as intended.

Tommie W. Kelley, et al. (3M), *Chem. Mater.* 2004, *16*, 4413-4422

RFID Market

Korea (단위 : 억 달러)

구분 \ 연도	2003	2004	2005	2006	2007	2008	2009	GAGR
태그	5.3	7.2	10.0	13.4	18.2	24.5	34.1	36.9%
리더기	2.7	3.8	5.3	7.0	9.5	12.7	17.7	37.4%
S/W&Service	3.0	4.0	4.0	7.6	10.3	13.8	19.2	36.9%
합계	11	15	21	28	38	51	71	37.1%

*자료 : IDC 2004.

World (단위 : 억원)

구분 \ 연도	2003	2004	2005	2006	2007	2008	2009	GAGR
태그	317	408	504	672	912	1,224	1,704	33.5%
리더기	165	213	262	350	475	637	888	33.5%
S/W&Service	178	229	284	378	513	689	958	33.6%
합계	660	850	1,050	1,400	1,900	2,550	3,550	33.5%

*자료 : 세계시장의 5%로 국내시장을 추정.

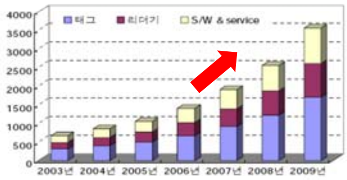

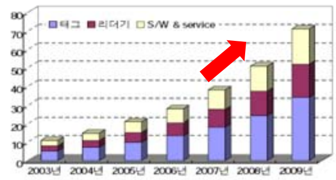

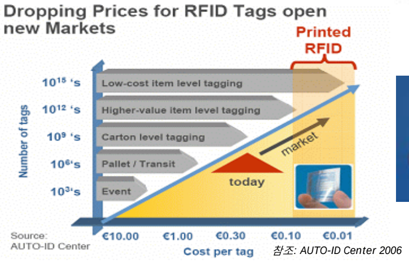

참조: AUTO-ID Center 2006

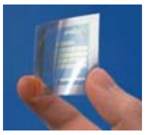

PolyIC www.polyic.com

Integrated circuits using OTFTs

Organic Semiconductor
EE 4541.617A
2009. 1st Semester

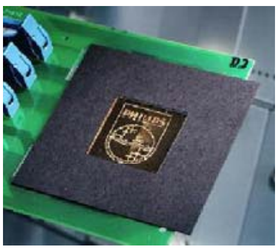

Philips Research: The 1st Polymer Dispersed Liquid Crystal (PDLC) display based on an organic TFT active matrix (August 2000).

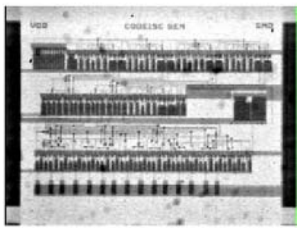

Philips Research: The 1st IC built using exclusively organic materials and containing over 300 transistors.
C.M. Hart, D.M. de Leeuw, M. Matters, P.T. Herwig, C.M.J. Mutsaerts and C.J. Drury, "Low cost all-polymer integrated circuits", *Proceedings of the ESSCIRC 98*, Sept. 1998, pp. 30-34.

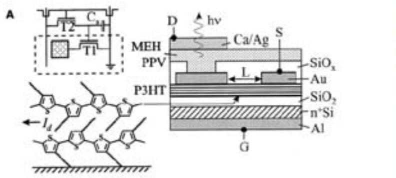

Fig. 1. (**A**) Cross section of the integrated P3HT FET and MEH-PPV LED. The device is a part (shown inside the dashed area in the top left corner) of a full active-matrix polymer LED pixel. The lamellar structure of the regioregular P3HT and its orientation relative to the SiO_2 substrate and the direction of the in-plane FET current I_d are shown schematically. (**B**) Photograph of a FET-LED with one of the four "pixels" switched on. The MEH-PPV layer (orange) was made to cover the substrate only partially in order to make the underlying (bluish) P3HT layer visible.

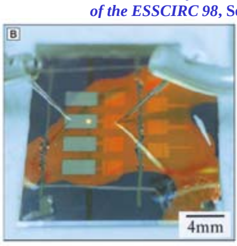

H. Sirringhaus, N. Tessler, R. H. Friend, Science 280, 1741 (1998)